Artificial Neural Network-Based Compensation for Transceiver Nonlinearity in Probabilistic Shaping Systems

Tu T. Nguyen*, **Tingting Zhang, Mahmood Abu-Romoh and Andrew Ellis**

Aston Institute of Photonic Technologies, Aston University, Birmingham, B4 7ET, United Kingdom

**t.nguyen14@aston.ac.uk*

Abstract: Artificial neural network for transceiver nonlinearity compensation in dual-polarization probabilistically shaped 28 GBaud systems is experimentally investigated with achieved SNR performance gain up to 1 dB. © 2020 The Author(s)

OCIS codes: (060.2330) Fiber optics communications; (060.4080) Modulation

1. Introduction

High-order quadrature amplitude modulation (QAM) formats combined with probabilistic shaping (PS) technique have attracted a lot of attention in recent years. It enables at the same time high spectral efficiency (SE) and flexible transmissions [1–3]. With the PS technique, adaptable transmission rates can be realized by adjusting the shaping factor without forward error correction (FEC) modification [2, 4].

Generally, the implementation of high-order modulation formats such as such as 64-QAM and beyond is often a big challenge due to the requirement on high signal-to-noise ratio (SNR), high effective number-of-bit of digital-to-analog converters (DACs) and analog-to-digital converters (ADCs), and good transceiver linearity, which yet is practically limited by the imperfection of transceiver devices such as power amplifiers and optical modulators. Thus, the nonlinear distortion is unavoidable in practical systems. The nonlinear distortion from the transceiver can be compensated by using digital filters [5, 6]. Nevertheless, it is difficult to estimate exact coefficients of these filters as the result of the nonlinear mixing from different devices of the transceivers, especially in a mesh optical network. To partly deal with this problem, a recent machine-learning-based technique namely artificial neural network (ANN) has been applied numerically for 64-QAM systems as a pre-distortion compensation [7]. However, this work only focus on the low resolution DAC at the transmitter side and ignore nonlinear contributions from other components for a practical system.

The above-mentioned problem is predicted even more severe with the probabilistically shaped signals which can be seen through the merit of peak-to-average power ratio (PAPR) in the third section. In this paper, we have proposed, for the first time, the application of ANN for compensating coupled-nonlinear distortions from the transceivers in PS systems. The proposed scheme was taking place at the receiver and experimentally verified for dual polarization (DP) probabilistically shaped 28 GBaud 64/256 QAM transmissions. Experimental results show that up to 1 dB SNR improvement can be obtained with ANN-aided nonlinear compensation (NLC) for such PS systems.

2. System Description and Experimental Setup

The experimental setup of a 28 GBaud DP shaped 64/256-QAM back-to-back system is shown in Fig. 1. At the transmitter, we deployed a probabilistic amplitude shaping (PAS) scheme with Maxwell-Boltzmann (MB) distribution for probabilistically squared M-QAM generation [8]. The core element of the PAS architecture is a distribution matching algorithm in which a desired constellation distribution can be created from information bits. Square-shaped M-QAM symbols was generated by combining two independently shaped $\sqrt{M}$-pulse amplitude modulation (PAM) sequences which represent the real and imaginary components of their complex M-QAM symbols. In this work, the nearly-optimum shaping factors were chosen from a ready-to-use table in [9] in which a fixed probability mass function (PMF) can be used for a wide range of SNR with a negligible penalty (less than 0.1 dB SNR). From Table 1 [9], there are only two nearly-optimal sets of PMF for each modulation format, and we denote them as "ps-r1" and "ps-r2", respectively in this paper. Their corresponding entropy in bit-per-symbol, ($\mathbb{H}_{r1}$, $\mathbb{H}_{r2}$), for PS 64 and 256-QAM systems were (5.656, 4.910) and (7.572, 6.788), respectively. 10 % 4-QAM pilots were multiplexed with the shaped signals (i.e. 1 pilot in every 10 symbols) to aid digital signal processing (DSP) algorithms at the receiver (both channel equalizer and phase noise compensation). The power of pilot symbols was scaled to be as the same as the power of the shaped signal. A root-raised-cosine (RRC) filter with a roll-off factor of 0.1 was then applied for the shaped QAM off-line, loaded into an arbitrary waveform generator (4-channel 8-bit sampling at 56 GSa/s) and subsequently converted into the optical domain by using a conventional DP optical coherent transmitter. To vary the received SNR, the DP optical signal was connected to a variable optical attenuator followed by an Erbium-doped fiber amplifier (EDFA) before going to the coherent reception.

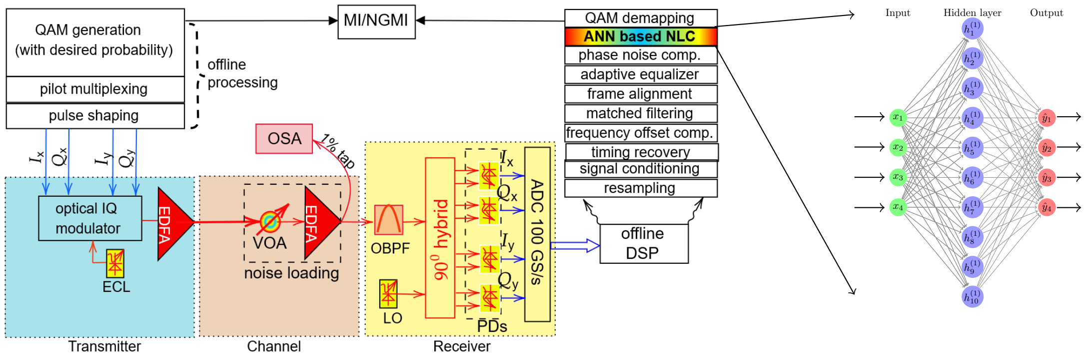

Fig. 1. Experimental setup for dual polarization probabilistically shaped 28 GBaud 64/256-QAM systems. (Inset) artificial-neural-network-based nonlinear compensation (ANN-based NLC). ECL: External cavity laser, EDFA: Erbium-doped fiber amplifier, VOA: Variable optical attenuator, OBPF: Optical bandpass filter, LO: Local oscillator, PDs: Photodetectors, OSA: Optical Spectrum Analyzer.

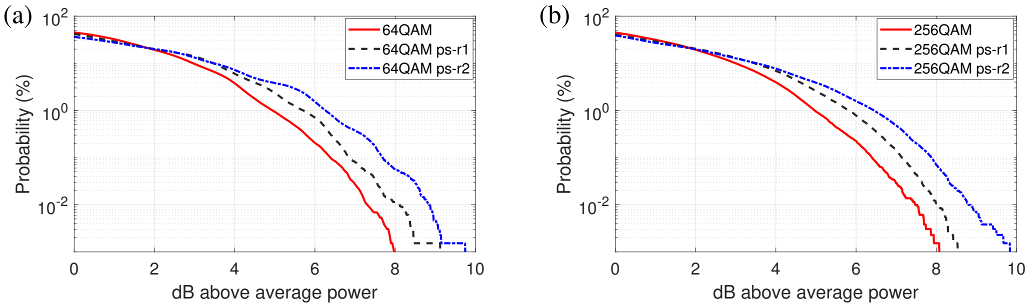

Fig. 2. PAPR comparison of QAM signal with and without probabilistic shaping. (a): 64-QAM, (b): 256-QAM

At the receiver, the optical signal was first converted into electrical signals by a local oscillator (LO), 90^o hybrid and four pairs of balanced photo-detectors. The electrical signals were captured and digitized by a real-time oscilloscope with 8-bit sampling at 100 GSa/s before offline processing. The off-line DSP started with the resampling to 2 samples per symbol. Then, the digital signals were formatted/scaled by a signal conditioning module. Before the matched-filtering, the timing recovery and frequency offset error correction based on a Gardner phase detector and a conventional Fourier-transform-based method, respectively were performed. A pilot-aided channel equalizer based on a 21-tap constant-modulus algorithm was then carried out to cancel any linear effects. The phase noise was estimated and compensated by using a conventional pilot-aided method (using 8 pilots in each block of 71 symbols for a sufficient noise averaging). Before QAM de-mapping, the ANN-based NLC was used to equalize the nonlinear impairment from transceivers.

As a supervised learning scheme, the ANN-based NLC was operated in two modes: training and testing mode. In the training mode, all neural network parameters were optimized thanks to Levenberg-Marquardt back-propagation algorithm with the aid of transmitted symbols. It aimed to minimize the error $e = \mathbb{E}\{\boldsymbol{y} - \boldsymbol{x}\}^2$, where $\boldsymbol{y}$ and $\boldsymbol{x}$ were the received and transmitted QAM symbols respectively. A simple 4×4 feed-forward network with 10 neurons and 1 hidden layer was chosen to implement ANN based NLC as shown in Fig. 1 (inset). The activation function used in the hidden layer was hyperbolic tangent sigmoid transfer function, whereas 4 neurons of the output layer used linear transfer functions. After training, the inverted nonlinear function $f_{\rm nl}^{-1}(.)$ reflecting all coupled nonlinearities of the transceivers was carried out. In the operational (testing) mode, the received signals were compensated as $\hat{\boldsymbol{y}} = f_{\rm nl}^{-1}(\boldsymbol{y})$. We assumed that the nonlinear distortion from transceiver was static or time-slowly varying, the learning stage was therefore taking place one time at the best condition (highest SNR). This training process may be repeated periodically if necessary (during initialization/calibration stages, for example). The number of symbols for training phase was 2^{15} in which the ratios of 70 %, 15 % and 15 % were dedicated for the training, validation and testing, respectively.

3. Results and Discussion

To assess the performance of systems, we adopted the merit of normalized generalized mutual information (NGMI) which indicates the maximum number of information bits per transmit bit. The NGMI is the most reliable figure of merit to predict the post-FEC performance without the real FEC implementation [10]. NGMI thresholds used in this paper for all comparison are 0.67, 0.8 and 0.91 (the family of low-density parity-check code rates [10]). For each SNR, NGMI was calculated from around 59 000 shaping-transmitted symbols.

First of all, Fig. 2 shows the PAPR comparison between QAM signal with and without the constellation shaping

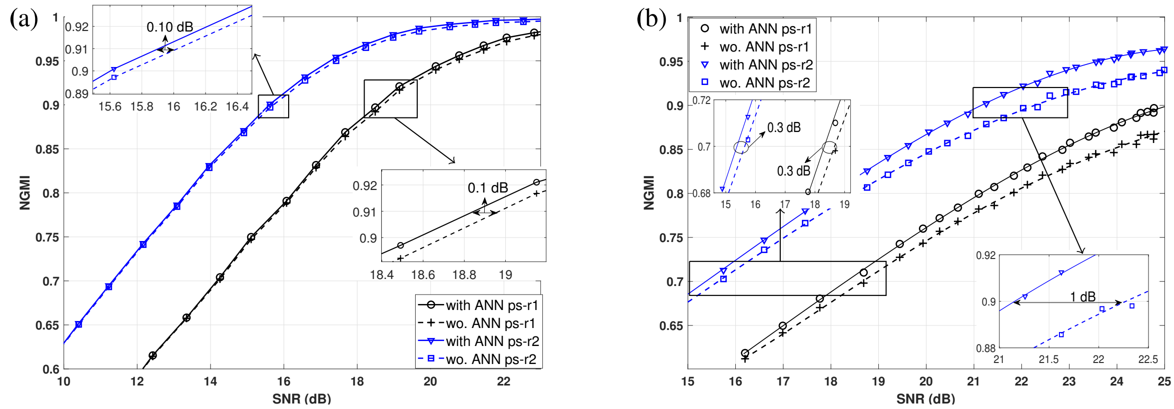

Fig. 3. NGMI performance of the probabilistically shaped dual-polarization 28 GBaud transmissions with and without the ANN-based NLC as a function of SNR under different shaping rates ("ps-r1" and "ps-r2"): (a): shaped 64-QAM and (b): shaped 256-QAM.

after pulse shaping. For each modulation format, two shaping rates as mentioned in the section 2 were considered for the comparison. The vertical axis is the complementary cumulative distribution function showing how often a certain PAPR in the horizontal axis is exceeded. As both figures show, the shaping signals exhibit larger PAPR than the unshaped ones and the more shaping, the worse PAPR. Specifically, at the same probability of 1 %, PAPRs increase by 0.7 dB and 1.5 dB with the shaping rates of ps-r1 and ps-r2, respectively for 64 and 256 shaped-QAM in comparison with their unshaped counterparts. These increments indicate that linear operation ranges of transceiver devices such DAC/ADC, power amplifiers and modulators need to be increased as well. Otherwise, some nonlinear distortion may be introduced.

Fig. 3 shows the system's performance with and without ANN-based NLC in term of NGMI versus SNR for the DP probabilistically shaped 64/256-QAM back-to-back transmissions. For the shaped 64-QAM system (Fig. 3-(a)), at FEC threshold of 0.91, there is a little improvement for the system equipped with the nonlinear compensator, only around 0.1 dB SNR for both shaping rates ps-r1 and ps-r2 because the number of bits of DAC/ADC in this experiment was high enough to support this 64-QAM signal and the modulator was calibrated well. At other thresholds, no improvement was observed because the impairment was dominated by Gaussian noise.

On the other hand, the performance improvement the shaped 256-QAM system equipped with the ANN-based NLC is significant, as depicted in Fig. 3-(b). In this experiment, we kept the same setup as the above system but the order of the modulation format was increased from 64 to 256. The nonlinear distortion was therefore expected to increase. Thus, the improved performance with the aid of NLC in this experiment is more visible, as shown in this figure. Specifically, the SNR gains with the ANN-based NLC are around 0.3 dB, 0.7 dB and 1 dB for three above-mentioned FEC thresholds, respectively. More importantly, it can be seen that the NGMI improvement at a same SNR is larger for the case of ps-r2 in comparison with ps-r1, which shows a good agreement with previous conclusion that the deeper shaping imposes more nonlinear distortion from the transceivers.

4. Conclusion

We have experimentally shown an effectiveness of transceiver nonlinearity compensation based on ANN for the probabilistically shaped 64/256-QAM systems. A SNR gain of up to 1 dB was obtained for shaping systems equipped with our proposed scheme. The results also indicate that transceiver re-calibration may be needed when high-order shaped-QAM signals are present in the systems. Otherwise, additional DSP techniques like the ANN-based NLC are necessary to be deployed at the receiver to compensate nonlinear distortion from the transceivers.

Acknowledgements: This work was supported by the UK EPSRC - Grants EP/S003436/1, EP/R035342/1 & EP/M009092/1. The data underlying this publication can be found at http://researchdata.aston.ac.uk/439/

References

1. M. P. Yankov *et al.*, in "Proc. of OFC," (OSA, 2017), paper W2A.48.
2. G. Bocherer *et al.*, IEEE Trans. Commun. **63**, 4651–4665 (2015).
3. J. Cho *et al.*, J. Light. Technol. **37**, 1590–1607 (2019).
4. F. Buchali *et al.*, J. Light. Technol. **34**, 1599–1609 (2016).
5. Q. Wang *et al.*, Appl. Sci. **9**, 1758 (2019).
6. P. W. Berenguer *et al.*, J. Light. Technol. **34**, 1739–1745 (2016).
7. A.-R. Mahmood *et al.*, in "Proc. of ECOC," (OSA, 2019), paper Th.1.B.4.
8. P. Schulte *et al.*, "shapecomm WebDM." http://dm.shapecomm.de (2017).
9. T. Fehenberger *et al.*, J. Light. Technol. **34**, 5063–5073 (2016).
10. J. Cho *et al.*, in "Proc. of ECOC," (2017), paper M.2.D.2.